ELSEVIER

www.elsevier.nl/locate/jorganchem

Journal of Organometallic Chemistry 620 (2001) 202–210

Journal of Organometallic Chemistry

Spectroscopy and photochemical reactivity of cyclooctadiene platinum complexes

Axel Klein [a,*], Joris van Slageren [b], Stanislav Záliš [c]

[a] *Institut für Anorganische Chemie, Universität Stuttgart, Pfaffenwaldring 55, D-70569 Stuttgart, Germany*
[b] *Institute of Molecular Chemistry, University van Amsterdam, Nieuwe Achtergracht 166, NL-1018 WV Amsterdam, The Netherlands*
[c] *J. Heyrovský Institute of Physical Chemistry, Academy of Sciences of the Czech Republic, Dolejškova 3, CZ-18 223 Prague 8, Czech Republic*

Received 16 June 2000; received in revised form 22 August 2000; accepted 10 October 2000

Abstract

The spectroscopic and photochemical properties of a series of 1,5-cyclooctadiene platinum complexes of the type $[(COD)Pt(R)_2]$ (R = alkyl, alkynyl, or aryl) were examined. The observed photoreactivity is wavelength dependent and observed reaction rates correlate with the donor-strength of the R group. For strongly donating substituents like adamantylmethyl, benzyl or *iso*-propyl rates were increased by factors of about 100 for a given model reaction compared to the dimethyl derivative. The products were determined by NMR spectroscopy. Different reaction pathways were found depending on the substituents R. Theoretical calculations (DFT) on the electronic structure revealed the character of optical transitions and excited states. © 2001 Elsevier Science B.V. All rights reserved.

Keywords: Cyclooctadiene platinum complexes; Photochemistry; Photophysics; Optical spectroscopy; Theoretical calculations; DFT

1. Introduction

Organoplatinum(II) complexes $[(COD)Pt(R)_2]$ (R = alkyl or aryl) have been known since decades and are widely used as precursors for mono- and polynuclear organometallic platinum(II) compounds [1–9]. They are also of interest for the generation of organoplatinum reaction centres on catalyst surfaces for heterogeneous catalysis [10] or as potential precursors for chemical vapour deposition (CVD) of platinum [11]. Furthermore, in a preliminary communication Vogler and Kunkely reported that $[(COD)Pt(Me)_2]$ is photoreactive and undergoes photochemically initiated addition of methyl iodide to form $[(COD)Pt(Me)_3I]$ with $\Phi = 0.005$ at $\lambda_{irr} = 313$ nm [12]. Theoretical calculations on related systems have shown that the concerned highest occupied molecular orbital (HOMO) has contributions from the methyl substituents [12–16]. Our idea was that the photoreactivity should thus depend on the donor strength of the R substituent and that the reactivity might be enhanced using stronger donors than methyl. Therefore we prepared cyclooctadiene platinum(II) complexes with various substituents R and investigated their photochemical and spectroscopic properties. Assuming that the nature of the σ-donating orbital on the carbon atom (C_1) remains the same, the use of various substitutents at C_1 should result mainly in inductive effects (alkyl > aryl > silyl > H). Thus, compounds with tentatively stronger σ-donating substituents like $[(COD)Pt(^iPr)_2]$ (^iPr = *iso*-propyl) [17], $[(COD)Pt(adme)_2]$ (adme = 1-adamantyl-methyl) [9], $[(COD)Pt(neop)_2]$ (neop = neopentyl = 2,2-dimethyl-1-propyl) [18–20], $[(COD)Pt(neoPh)_2]$ (neoPh = neophyl = 2-methyl-2-phenyl-1-propyl) [21], $[(COD)Pt(neoSi)_2]$ (neoSi = neosilyl = trimethylsilylmethyl) [1,22,23] and $[(COD)Pt(Bzl)_2]$ (Bzl = benzyl) [1] were prepared and examined. Comparison is drawn to the 'standard' compound $[(COD)Pt(Me)_2]$ (Me = methyl) [1,22,24]. We also included in our investigations the alkynyl complexes $[(COD)Pt(C{\equiv}C^tBu)_2]$ ($C{\equiv}C^tBu$ = 2,2-dimethyl-1-propynyl) [25] and $[(COD)Pt(C{\equiv}CPh)_2]$ ($C{\equiv}CPh$ = 2-phenyl-ethynyl) [26] and $[(COD)Pt(Ph)_2]$ (Ph = phenyl) [4,27]. The latter is expected to be unreactive due to the lower σ donating ability.

* Corresponding author. Tel.: +49-711-6854235; fax: +49-711-6854165.
E-mail address: klein@iac.uni-stuttgart.de (A. Klein).

PII: S0022-328X(00)00792-0

Table 1
Selected ^{1}H-NMR data of COD and complexes [(COD)Pt(R)$_2$] [a]

Compound	δ (=CH)	^2JPt=CH	^2JPtCH$_n$
[(COD)Pt(Cl)$_2$]	5.53	72.6	
[(COD)Pt(C≡CPh)$_2$]	5.64	45.6	
[(COD)Pt(C≡C^{t}Bu)$_2$]	5.34	43.8	
[(COD)Pt(Me)$_2$]	4.75	41.1	82.2
[(COD)Pt(neoSi)$_2$]	4.65	41.1	93.6
[(COD)Pt(Bzl)$_2$]	4.61	40.8	114.9
[(COD)Pt(Ph)$_2$]	5.05	39.0	(14.9) [b]
[(COD)Pt(neop)$_2$]	4.89	37.5	92.4
[(COD)Pt(neoPh)$_2$]	4.09	37.5	89.4
[(COD)Pt(adme)$_2$]	4.83	37.5	92.4
[(COD)Pt(^{i}Pr)$_2$]	4.86	36.9	96.6

[a] From measurements at 300 MHz in CD_2Cl_2, chemical shifts δ in ppm vs. TMS, coupling constants to the ^{195}Pt isotope ($I = 1/2$, 33.8% nat. abundance) in Hz.
[b] Coupling of the *ortho*-H to ^{195}Pt.

Table 2
Observed electronic absorption maxima for complexes [(COD)Pt(R)$_2$] [a]

R	λ (4)	λ (3)	λ (2)	λ (1)
Ph [b]	273 (4520) [c]	305 (2950)	328 (1400)	365 (600)
C≡C^{t}Bu [b]	272 (3320)	286 (720)	307 (3240)	345 (650)
C≡CPh [b]	255 (4970)	280 (1180)	325 (3170)	359 (580)
	MLCT II	SBLCT II	MLCT I	SBLCT I
Me	248 (2600)	290 (1400)	318 (700)	358 (140)
NeoSi	251 (2570)	286 (1260)	319 (560)	361 (140)
NeoPh	253 (14 700) [d]	288 (10 430) [d]	327 (550)	380 (130)
Neop	266 (3490)	292 (1630)	336 (700)	386 (120)
Adme	260 (3860)	284 (1410)	338 (660)	385 (160)
Bzl	249 (15 100) [d]	282 (11 770) [d]	334 (980)	368 (170)
^{i}Pr	260 (2540)	295 (1230)	340 (720)	395 (150)

[a] From measurements in CH_2Cl_2. Absorption maxima (in nm), extinction coefficients (in M^{-1} cm^{-1}) in parentheses.
[b] For assignments see text.
[c] Further maxima at 314 nm (2810), 285 nm (3220) and 268 nm (4960).
[d] Assigned to π–π^* transitions of the phenyl cores.

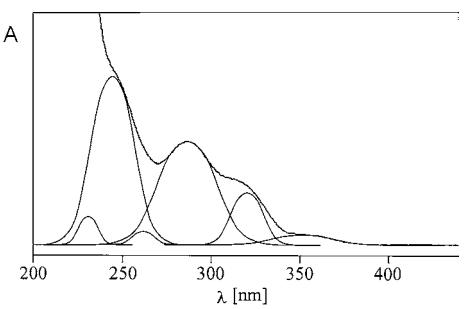

Fig. 1. Absorption spectrum of [(COD)Pt(Me)$_2$] in MeCN solution and spectral deconvolution.

Theoretical calculations using DFT techniques should enable unambiguous assignment of the electronic levels responsible for the electronic transitions and photoreactivity.

2. Results and discussion

2.1. Synthesis and characterization of the compounds

The complexes [(COD)Pt(R)$_2$] were prepared from [(COD)Pt(Cl)$_2$] using published procedures in the cases of [(COD)Pt(adme)$_2$] [9], [(COD)Pt(Bzl)$_2$], [(COD)-Pt(Me)$_2$], [(COD)Pt(neoSi)$_2$] [1], and [(COD)Pt(Ph)$_2$] [27]. The compounds [(COD)Pt(^{i}Pr)$_2$], [(COD)Pt-(neop)$_2$], [(COD)Pt(C≡C^{t}Bu)$_2$] and [(COD)Pt(C≡CPh)$_2$] were obtained by modified reaction procedures (see Section 4). All compounds were obtained in high yields. In case of the tentatively more strongly σ-donating substituents R = ^{i}Pr, neop, or adme, care was taken to avoid light during the preparation and isolation of the products, which was obviously beneficial for the yields.

The ^{1}H-NMR spectra of all the complexes show the typical broad resonance for the COD olefinic protons that exhibits satellites due to coupling of the protons with the ^{195}Pt isotope (^{195}Pt, $I = 1/2$, 33.8% nat. abund.). As was shown previously the ^2JPt–HC(olefin) coupling constant is a good probe for the donor strength of the *trans* located substituent R. Small coupling constants should go along with high donor strength of R as inferred from inductive effects [28]. The data obtained for the present complexes (Table 1) reveal that indeed the coupling constant is increasing on going from methyl to stronger R groups.

2.2. Optical spectroscopy and calculations

The absorption spectra for all the complexes show several maxima in the region from 250 to 400 nm (Table 2). The assignments of the main transitions were based on calculations on the characters of ground and excited states for [(COD)Pt(Me)$_2$], [(COD)Pt(^{i}Pr)$_2$], [(COD)Pt(Ph)$_2$], and the model complex [(COD)Pt(C≡CH)$_2$]. Spectral deconvolutions as shown in Fig. 1 for [(COD)Pt(Me)$_2$] were always in excellent agreement to these calculations.

The relative positions and compositions of selected [(COD)Pt(Me)$_2$] MOs are listed in Table 3. The lowest unoccupied MO (11b$_1$, Fig. 2) can be characterized as a π antibonding MO of the COD ligand with contributions of the p and d orbitals of the central Pt atom. The occupied MOs are to a large extent formed by d orbitals of Pt interacting with R and COD orbitals. Fig. 3 depicts the highest occupied molecular orbital, 16a$_1$, with relatively large contributions from the methyl sub-

Table 3
ADF calculated one-electron energies and percentage composition of selected highest occupied and lowest unoccupied molecular orbitals of [(COD)Pt(Me)$_2$] expressed in terms of composing fragments

MO	E (eV)	Prevailing character	Pt	Me	COD
Unoccupied					
$13b_2$	−0.21	d_{Pt} + Me + COD	2(p); 29(d)	48	23
$8a_2$	−0.71	π* COD	12(d)		88
$11b_1$	−1.71	π* COD	11(p); 13(d)	4	72 (π*)
Occupied					
$16a_1$	−5.01	d_{Pt} + Me + COD	15(s); 2(p); 40(d)	31	12 (π)
$15a_1$	−5.88	d_{Pt}	1(s); 79(d)	13	6
$12b_2$	−6.01	π_{COD} + Me	5(p); 4(d)	34	56
$7a_2$	−6.19	d_{Pt}	72(d)	11	16
$14a_1$	−6.28	d_{Pt} + Me + COD	4(p); 41(d)	20	34
$10b_1$	−6.29	d_{Pt}	1(p); 69(d)	9	20

stituents. The lower lying MO $12b_2$ is mainly delocalized over the COD and CH_3 ligands, while $15a_1$ can be described as a mainly metal localized molecular orbital. Both ADF/BP and G98/B3LYP calculations give qualitatively similar MO schemes.

The excited states calculations, performed for [(COD)Pt(Me)$_2$], gave a detailed picture of the various transitions (Table 4). The data are in excellent agreement with the absorption maxima found including relative intensities represented by the extinction coefficients. The character of the long-wavelength transition is thus of $\sigma_{(Pt-CH3)} \rightarrow \pi^*_{(COD)}$ sigma-bond-to-ligand charge transfer (SBLCT) character. Such a transition can be considered as a special case of a ligand-to-ligand charge transfer (LLCT) transition. However, the orbital that the SBLCT transition originates from, has sigma bonding character, while the accepting orbital is often of π* type. One consequence of this electronic transition is in general that complexes with a low-lying SBLCT state are photoreactive, due to removal of electron density from a bonding orbital.

The SBLCT transition is followed by a stronger band of $d\pi_{(Pt)} \rightarrow \pi^*_{(COD)}$ (MLCT) character. Generally the long-wavelength maxima exhibit slightly negative solvatochromism and increasingly shift to lower energies as the substituents R get stronger σ donors e.g. $\lambda_{max} = 360$ nm for Me and $\lambda_{max} = 390$ nm for ^{i}Pr. Calculations for the system with R = ^{i}Pr gave approximately the same picture as for R = Me (Table 5) indicating that the overall character of the excited states is the same for all dialkyl complexes. The transition energies calculated for R = ^{i}Pr gave 3.13 eV (osc. str. 0.003) for the long-wavelength absorption $^1B_1$, compared to 3.61 eV (0.002) for R = Me. The second transition $^1B_1$ is calculated at 4.03 eV (0.004) for R = ^{i}Pr and 4.46 eV (0.001) for R = Me. This supports the observed bathochromic shift of the long-wavelength transition for compounds containing substituents R that are stronger σ-donators than methyl.

In contrast to the dialkylplatinum complexes the long-wavelength maxima for [(COD)Pt(Ph)$_2$] are of different nature. A major difficulty for the calculations was the assignment of the tilt angle of the phenyl groups since this turned out to be crucial for the electronic structure. The tilt angle found in a crystal structure of [(COD)Pt(Ph)$_2$] is 82° [29]. However we obtained the best results assuming a tilt angle of 60° which might be explained by the fact that the crystal

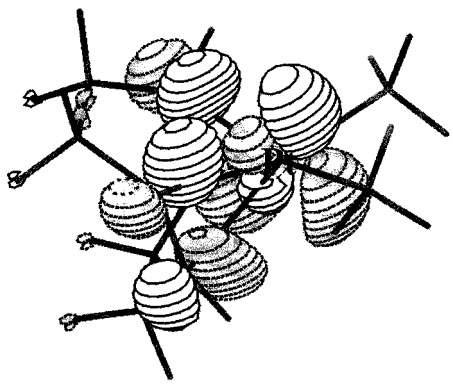

Fig. 2. $11b_1$ LUMO of [(COD)Pt(Me)$_2$].

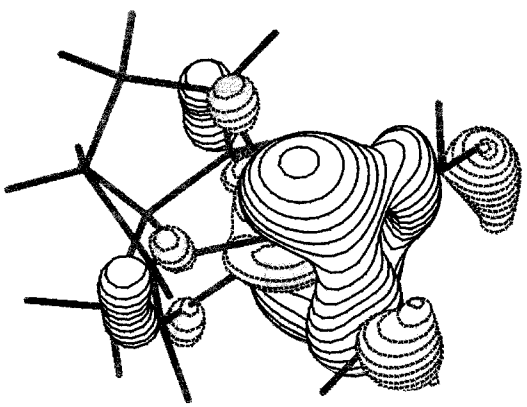

Fig. 3. $16a_1$ HOMO of [(COD)Pt(Me)$_2$].

Table 4
TD DFT calculated lowest singlet excitation energies (eV or nm), oscillator strengths and observed absorption maxima for $[(COD)Pt(Me)_2]$ [a]

State	Composition	Transition energy in eV (nm)	Osc. str.	Absorption max. found (ε) [b]	Absorption max. found (ε) [c]
$^1B_1$	98% ($16a_1 \rightarrow 11b_1$)	3.61 (343)	0.002	358 (140)	352 (150)
$^1B_1$	98% ($15a_1 \rightarrow 11b_1$)	4.36 (284)	0.001	318 (700)	318 (790)
$^1B_1$	91% ($14a_1 \rightarrow 11b_1$)	4.78 (260)	0.022	290 (1400)	286 (1340)
$^1B_2$	82% ($7a_2 \rightarrow 11b_1$); 14% ($16a_1 \rightarrow 13b_2$)	4.87 (254)	0.007	258 (110)	262 (170)
$^1A_1$	74% ($10b_1 \rightarrow 11b_1$); 10% ($7a_2 \rightarrow 8a_2$)	5.12 (242)	0.042	248 (2600)	248 (2350)
$^1A_1$	92% ($16a_1 \rightarrow 17a_1$)	5.23 (237)	0.005	242 (120)	237 (200)
$^1B_1$	82% ($12b_2 \rightarrow 8a_2$)	5.78 (214)	0.033	n.d. [d]	218 (13 000)
$^1A_1$	99% ($16a_1 \rightarrow 18a_1$)	5.89 (210)	0.011	n.d. [d]	202 (19 250)

[a] Maxima (in nm) and extinction coefficients (in M^{-1} cm^{-1}) were extracted form spectral deconvolution as shown in Fig. 1.
[b] In CH_2Cl_2 solution.
[c] In MeCN solution.
[d] Not detected due to absorption of the solvent.

Table 5
ADF calculated one-electron energies and percentage composition of selected highest occupied and lowest unoccupied molecular orbitals of $[(COD)Pt(^iPr)_2]$ expressed in terms of composing fragments

MO	E (eV)	Prevailing character	Pt	^{i}Pr	COD
Unoccupied					
$14b_1$	−1.91	π* COD	12(p); 16(d)	5	67 (π*)
Occupied					
$19a_1$	−4.82	$d_{Pt} + {}^iPr + COD$	18(s); 2(p); 29(d)	43	7 (π)
$15b_2$	−5.81	$\pi_{COD} + {}^iPr$	10(p); 4(d)	41	44
$18a_1$	−5.92	d_{Pt}	1(s); 75(d)	16	8
$10a_2$	−6.21	d_{Pt}	78(d)	13	8

structure represents the solid state whereas the calculation allows the system to optimize for an isolated molecule in the gas phase. The low energy maximum is found in the spectrum as a weak shoulder at 365 nm and we attribute this to the triplet absorption belonging to the lowest electronic transition. The tentative assignment is based on the fact that the calculated energy for the singlet transition is too high and such singlet triplet absorption are frequently observed for platinum complexes due to their large spin orbit coupling. The second lowest absorption maximum is assigned to the HOMO ($\pi/\sigma_{(phenyl)}$) → LUMO ($\pi^*_{(COD)}$) (34a → 34b) transition. The calculated maximum (Table 6) is ca. 3800 cm^{-1} too low. The contributions of platinum orbitals to the HOMO and the LUMO are each approx. 30%, so the overall character is a LLCT. Although the prevailing character of the contribution of the phenyl substituents can be described as π_{Phenyl} a sharp discrimination between σ or π is not possible since there are contributions of both types at the C_1 atom bound to platinum. A number of higher lying transitions were calculated and also observed as shown in Table 6. Their overall character is also best described as LLCT transition. This is in agreement with previous assignments based in part on CD-spectra [30–32].

The long-wavelength maxima of the two complexes $[(COD)Pt(C{\equiv}CR')_2]$ are at higher energies compared to $[(COD)Pt(Me)_2]$ and are accompanied by weak shoulders at the low-energy tail. Our calculations reveal that both HOMO and LUMO show ca. 20% contributions of platinum orbitals so the overall character is an LLCT transition (LLCT I). The intense band found at 307 nm (R′ = ^{t}Bu) or 325 nm (R′ = Ph) is thus assigned to the singlet HOMO–LUMO ($\pi_{(CCR')} \rightarrow \pi^*_{(COD)}$) transition, the shoulders observed red shifted to them are assigned to the corresponding triplet absorptions. Since the results for the transition energies using the ADF method were not fully satisfying we also embarked on G98/B3LYP type of calculations. The agreement with the observed energies is far better as can be seen in Table 7.

2.3. Photochemistry

The wavelength-dependence of the photoreactivity was monitored by absorption spectroscopy in CH_2Cl_2 or MeCN solution, examples are displayed in Figs. 4

Table 6
ADF calculated one-electron energies and percentage composition of selected HOMO and LUMO and TD DFT calculated lowest singlet excitation energies (eV or nm), oscillator strengths and observed absorption maxima for [(COD)Pt(Ph)$_2$] ($\alpha = 60°$) [a]

MO	E (eV)	Prevailing character	Pt	Ph	COD
Unoccupied					
35a	−1.51	π* COD	9(d)	5	75
34b	−2.56	π* COD + Pt	18(p); 9(d)	7	66 (π*)
Occupied					
34a	−5.69	$d_{Pt} + \pi_{Ph}$	8(s); 28(d)	52	11 (π)
33b	−5.90	π_{Ph}	1(p); 2(d)	87	9
33a	−5.96	$d_{Pt} + \pi_{Ph}$	7(s); 2(p); 36(d)	50	5
32a	−6.27	π_{Ph}		95	5
32b	−6.28	π_{Ph}	1(d)	94	5

State	Composition	Transition energy in eV (nm)	Osc. str.	Absorption max. found (ε)
^{3}B	91% (34a → 34b)	3.05 (406)		365 (600)
^{1}B	91% (34a → 34b)	3.30 (375)	0.022	328 (1400)
^{1}A	99% (33b → 34b)	3.45 (359)	0.042	314 (2810)
^{1}B	79% (33a → 34b)	3.57 (347)	0.010	305 (2950)
^{1}B	79% (34a → 35b)	4.59 (270)	0.011	285 (3220)
^{1}B	70% (30a → 34b)	4.85 (255)	0.016	273 (4520)
^{1}B	70% (34a → 37b)	4.91 (253)	0.016	268 (4960)

[a] Tilt angle of the phenyl substituent to the coordination plane. Maxima (in nm) and extinction coefficients (in M^{-1} cm^{-1}) as observed in CH_2Cl_2 solution.

Table 7
ADF calculated one-electron energies and percentage composition of selected HOMO and LUMO and TD DFT calculated lowest singlet excitation energies (eV or nm), oscillator strengths and observed absorption maxima [a] for [(COD)Pt(C≡CH)$_2$]

MO	E (eV)	Prevailing character	Pt	CCH	COD
Unoccupied					
$8a_2$	−1.37	π* COD	9(d)	9	89
$11b_1$	−2.52	π* COD	16(p); 8(d)	8	59 (π*)
Occupied					
$17a_1$	−5.51	π CCH + d_{Pt}	1(s); 19(d)	77	3 (π)
$7a_2$	−5.64	π CCH	11(d)	86	3
$13b_2$	−5.69	π CCH		96	4
$10b_1$	−5.94	π CCH + d_{Pt}	2(p_x); 10(d)	78	10
$16a_1$	−6.21	d_{Pt}	10(s); 1(p); 68(d)	13	6

		G98/B3LYP		ADF/BP		
State	Composition	Transition energy in eV (nm)	Osc. str.	Transition energy in eV (nm)	Osc. str.	Absorption max. found (ε)
$^3B_2$ [b]	99% ($7a_2 \rightarrow 11b_1$)	[c]		2.98 (416)		345 (600)
$^1B_2$	96% ($7a_2 \rightarrow 11b_1$)	3.89 (310)	0.088	3.49 (355)	0.081	307 (3240)
$^1A_1$	88% ($10b_1 \rightarrow 11b_1$)	4.21 (294)	0.112	3.78 (328)	0.096	272 (3320)
$^1B_1$	98% ($16a_1 \rightarrow 11b_1$)	4.29 (289)	0.005	3.98 (310)	0.005	286 (720)

[a] Maxima (in nm) and extinction coefficients (in M^{-1} cm^{-1}) as observed for [(COD)Pt(C≡C^{t}Bu)$_2$] in CH_2Cl_2 solution.
[b] Alternative assignment $^1B_1$ [98% ($16a_1 \rightarrow 11b_1$)]; 3.51 eV (353); 0.0001 (G98/B3LYP calc.).
[c] Triplet transitions were not calculated in G98.

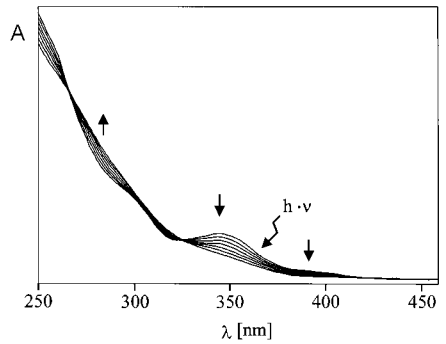

Fig. 4. Absorption spectra of [(COD)Pt(^{i}Pr)$_2$] taken in CH_2Cl_2 during photolysis at $\lambda > 360$ nm. The traces are recorded after each 20 s of irradiation. The last trace represents the spectrum of [(COD)Pt(^{i}Pr)Cl].

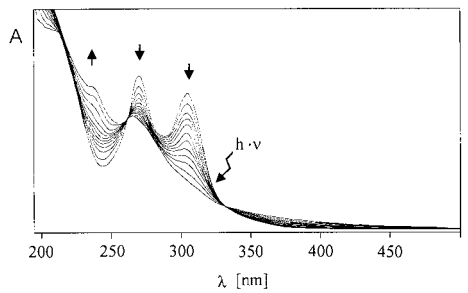

Fig. 5. Absorption spectra of [(COD)Pt(C≡C^{t}Bu)$_2$] taken in MeCN during photolysis at $\lambda > 320$ nm. The traces are recorded after each 20 s of irradiation.

and 5. We found that irradiation into the long-wavelength bands results in photodecomposition for the dialkyl and dialkynyl complexes. Irradiation at higher energy does not change the photoreactivity markedly. We could neither find intermediate regions of no photoreactivity nor markedly enhanced reactivity. This is in agreement with our assignments of the different optical transitions that occur in these compounds (SBLCT, MLCT or LLCT).

The relative reactivities of the different compounds in one chosen model reaction (Table 8) were examined by irradiation of concentrated solutions in CD_2Cl_2 and monitoring the reactions by ^{1}H-NMR spectroscopy. Also the identification of photoproducts was effected from these solutions. We followed the decay of the starting material and the reaction rates are compared to that of [(COD)Pt(Me)$_2$].

For a series of experiments using a constant irradiation wavelength $\lambda > 320$ nm we found increasing reaction rates for the dialkyl complexes along the series Me < neoSi < neoPh < neop < ^{i}Pr < adme < Bzl, the last two by a factor of 100. The above series fits very well to the donor strength of the R group as expected from inductive effects. Comparison of these rates lacks from the fact, that we did not use monochromatic light but band irradiation. However, the wavelength dependence of the photoreactivity is assumed to be small. Quantitatively this can be inferred from an experiment with [(COD)Pt(Me)$_2$] using higher energetic light ($\lambda >$ 295 nm). The rate found here is increased only by a factor of 1.7. The wavelength dependence may also account for the finding that adamantylmethyl and benzyl exhibit a higher rate than *iso*-propyl. This is contrary to expectation since the last represents the strongest donor substituent in the series investigated here. The observed enhancement of the photoreactivity is in excellent agreement to the calculations. Comparison of the photoreactive SBLCT states for R = Me and R = ^{i}Pr (Tables 3 and 5) reveals that the contribution of the substituents R to the HOMO increases from 31 (for Me) to 43% for ^{i}Pr in agreement with the higher photoreactivity.

The rates for the dialkynyl complexes are found to be higher than for the dimethyl derivative. However, the different type of excited states precludes a direct comparison. With the same setup the phenyl derivative [(COD)Pt(Ph)$_2$] was found to be unreactive.

The main photoproducts were identified by ^{1}H- or ^{13}C-NMR in the reaction mixtures in comparison to independently prepared authentic samples. For substituents R = ^{i}Pr, Bzl, adme, neop, neoPh and neoSi, these were the mono-chlorinated platinum complexes [(COD)PtRCl], the R–R coupling products and some chlorinated hydrocarbons (reaction 1, in Scheme 1). The monochlorinated products are further photolyzed under these conditions to yield the dichloro complex [(COD)Pt(Cl)$_2$] in high yields (60–80%). For the dimethyl derivative the monochlorinated species is found only in small amounts, the main product is the dimethylated saturated hydrocarbon 1,5-dimethylcyclooctane (reaction 3).

For the alkynyl derivatives the reaction occurs in a very clean fashion giving only the R–R coupling product, COD and elemental platinum (reaction 2).

Table 8
Relative rates of photodecomposition reactions in CD_2Cl_2 using cut-off filter $\lambda > 320$ nm

R	Ph	C≡C^{t}Bu	C≡CPh	Me	Me [a]	neoSi	neoPh	neop	^{i}Pr	adme	Bzl
k_{rel}	– [b]	3.7	1.13	1	1.67	10.7	42	51	86	111	120

[a] Cut-off filter $\lambda > 295$ nm.
[b] No reaction observed.

The reactivity of the alkyl derivatives can be easily understood assuming the homolytic cleavage of one Pt–R bond. The resulting radical pair dissociates, the platinum radical takes up a chlorine from the solvent and the alkyl radicals •R combine with another •R or with the solvent. The methyl radical, however, is expected to be much more reactive than the other •R radicals and thus, before leaving the solvent cage, obviously reacts with the CODPt fragment (cage reaction). The reaction presumably occurs at the double bonds and further steps involve the cleavage of platinum and the saturation of the olefin groups.

The alkynyl derivatives react in a very different manner. The product formation is reminiscent of the photoelimination of biaryl from bis(aryl)platinum compounds [31–34] or related concerted pericyclic reactions [35]. The occurrence of this type of reaction only for complexes where the R substituent contains a π system that is involved in the optical transitions, is a strong argument for the so-called π-mechanism to occur in these reactions. In the present systems the uptake of a photon promotes electron density from the π systems of the R substituent to π* orbitals mainly centered at the COD ligand and thus initiates the formation of a three-membered ring (pericyclic) transition state involving π orbitals at the C_1 atoms of both substituents R. In other words, the transition state might be favored through the formal electron promotion. Due to the different reaction mechanisms the relative reaction rates found for the dialkynyl complexes can thus not be compared to the dialkyl systems.

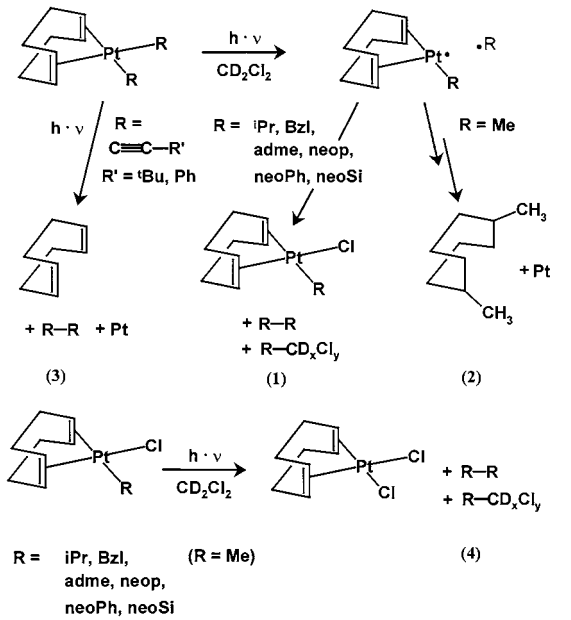

Scheme 1. Proposed reaction scheme for photochemical reactions of complexes [(COD)Pt(R_2)].

3. Conclusions

The optical transitions of complexes of the type [(COD)Pt(R_2)], R = alkyl, alkynyl or phenyl were determined with high accuracy by absorption spectroscopy, spectral deconvolution and quantum–chemical calculations. The theoretically predicted energies and intensities were in excellent agreement with observed maxima and extinction coefficients for the dialkyl complexes. The ADF/BP calculated values for the dialkynyl complexes or the diphenyl derivatives are only of moderate commensurability with the found ones. Excellent results were obtained for the model system [(COD)Pt($C{\equiv}CH)_2$] on G98/B3LYP type of calculations. Unfortunately the size of [(COD)Pt($Ph)_2$] precludes such calculations.

The photochemical reactivity of these electron rich dialkyl COD platinum(II) complexes can be dramatically increased by the replacement of methyl by stronger substituents like benzyl, adamantylmethyl or *iso*-propyl. The rate for a chosen model reaction is 100 times bigger for the latter derivatives. Our semi-quantitative method to assess relative reaction rates gave reliable results since the wavelength-dependence of the photoreactivity is minor compared to the enormous changes induced by different substituents R. For the dialkyl complexes the photochemical initial step is very probable the cleavage of a platinum–carbon bond and the formation of alkyl radicals. The reactivity and the reaction pathways are again in good agreement with the results from the calculations. The lowest absorption can be unambiguously assigned to a photoreactive SBLCT excited state. Replacing methyl by stronger alkyl donors leads to decreased transition energies and higher contributions of the substituents R to the HOMO. Thus higher photoreactivity is induced. The low-energy SBLCT excited state should enable a variety of photochemical reactions and further work is warranted and ongoing. One aspect will be the use of the photochemically prepared alkyl radicals. Alkynyl derivatives were also found to be quite reactive, however, in contrast to the dialkyl derivatives the reaction occurs in a concerted pericyclic way giving the diacetylenes, COD and platinum. Their reactivity might be used for photo-initiated deposit of platinum on surfaces or as heterogeneous catalysts.

4. Experimental

4.1. Instrumentation

^{1}H-NMR spectra for analytical purposes were recorded on a Bruker AC 250 spectrometer. The photoreactions were performed by irradiation of solutions in CD_2Cl_2 (Cambridge Isotope Laboratories, 99.9% D) with an Oriel 6137 high pressure Hg lamp. These

photoreactions were monitored by NMR (Varian Mercury 300). The relative rate constants of the photoreactions were determined by fitting the decay of the integral of the COD olefin signal of the starting com-pound with time to a mono-exponential function. UV–vis absorption spectra were recorded on a Bruins Instruments Omega 10, a Hewlett–Packard 8453 Diode Array or Varian Cary 4E spectrometer.

4.2. Materials

[(COD)Pt(adme)$_2$] [9], [(COD)Pt(Bzl)$_2$], [(COD)Pt-(Me)$_2$], [(COD)Pt(neoSi)$_2$], [(COD)Pt(Cl)$_2$] [1], and [(COD)Pt(Ph)$_2$] [27], were prepared according to published procedures. A sample of [(COD)Pt(neoPh)$_2$] was obtained from Colonial Metals Inc.

4.2.1. Synthesis of [(COD)Pt(^{i}Pr)$_2$]

A total of 935 mg of [(COD)Pt(Cl)$_2$] (2.5 mmol) were suspended in 25 ml of dry diethyl ether and cooled to −50°C. Then 25 ml of a Grignard solution prepared from 413 mg magnesium turnings (17 mmol) and 1.845 g of 2-bromopropane (15 mmol) in diethyl ether were added slowly under protection from light. The suspension was allowed to warm up to −40°C, then 3 ml of COD were added and the reaction mixture was stirred for 3 h. At −50°C, 5 ml of methanol were added, giving an off-white precipitate. After removal of all volatiles, the brownish residue was extracted with five 10-ml portions of pentane. Evaporation of the solvent from an ice cold bath under the protection from light gave 545 mg (1.4 mmol, 56%) off-white product. Anal. Calc. for $C_{14}H_{26}Pt$ (M_W: 389.45 g mol^{-1}): C, 43.18; H, 6.73. Found: C, 43.08; H, 6.59%.

^{1}H-NMR ($CDCl_3$): δ 4.88 (s, 4H, ^2J(Pt–CH=) = 36.4 Hz), 2.43–2.13 (m, 8H), 1.69 (sept, 2H, ^2J(Pt–CH) = 96.4 Hz), 1.16 (d, 12H, ^3J(Pt–CCH$_3$) = 69.9 Hz).

4.2.2. Synthesis of [(COD)Pt(neop)$_2$]

A total of 935 mg of [(COD)Pt(Cl)$_2$] (2.5 mmol) were suspended in 25 ml of dry diethyl ether and cooled to −80°C. Then 25 ml of a Grignard solution prepared from 413 mg magnesium turnings (17 mmol) and 2.265 g of bromo-2,2-dimethylpropane (15 mmol) in diethyl ether were added slowly under protection from light. The suspension was allowed to warm up to ambient temperature and stirred for 4 h at ambient temperature under the protection from light. At −50°C 5 ml of methanol were slowly added to give an off-white precipitate. After stirring for 1 h at ambient temperature, all volatiles were removed and the brownish residue was extracted with five 10-ml portions of pentane. Evaporation of the solvent from an ice cold bath under protection from light gave 835 mg (1.87 mmol, 75%) off-white product. Anal. Calc. for $C_{18}H_{34}Pt$ (M_W: 445.56 g mol^{-1}): C, 48.52; H, 7.69. Found: C, 48.61; H, 7.72%.

^{1}H-NMR (CD_2Cl_2): δ 4.88 (s, 4H, ^2J(Pt–CH=) = 37.5 Hz), 2.32–2.11 (m, 8H), 1.87 (s, 4H, ^2J(Pt–CH$_2$) = 92.4 Hz), 1.05 (d, 12H, ^4J(Pt–CCCH$_3$) = 4.2 Hz).

4.2.3. Synthesis of [(COD)Pt(C≡CPh)$_2$] and [(COD)Pt(C≡C^{t}Bu)$_2$]

A total of 935 mg of [(COD)Pt(Cl)$_2$] (2.5 mmol) were suspended in 60 ml of ethanol and cooled to −5°C. A total of 566 mg of potassium *tert*-butoxide (5.05 mmol) were dissolved in 20 ml of ethanol mixed with 5.1 mmol of the acetylene (521 mg phenylacetylene or 419 mg of 3,3-dimethyl-1-butyne) and transferred to a dropping funnel. After slow addition of this mixture to the reaction flask, the reaction was stirred at 10°C for 3 h after which the suspension had turned yellow. Evaporation of all volatiles and washing several times with small portion of pentane yielded slightly yellowish microcrystalline solids. Thus, 1175 mg of [(COD)Pt(C≡CPh)$_2$] (93%) were obtained. Further recrystallization was not necessary. Anal. Calc. for $C_{24}H_{22}Pt$ (M_W: 505.53 g mol^{-1}): C, 57.02; H, 4.39. Found: C, 57.13; H, 4.42%.

^{1}H-NMR (CD_2Cl_2): δ 7.41–7.32 (m, 4H, *o*-Ph), 7.25–7.09 (m, 6H, *m*-Ph, *p*-Ph), 5.64 (s, 4H, ^2J(Pt–CH=) = 46.0 Hz), 2.78–2.45 (m, 8H).

[(COD)Pt(C≡C^{t}Bu)$_2$] was obtained by this method in an amount of 1004 mg (95%). Anal. Calc. for $C_{20}H_{30}Pt$ (M_W: 465.55 g mol^{-1}): C, 51.60; H, 6.50. Found: C, 51.79; H, 6.69%.

^{1}H-NMR (CD_2Cl_2): δ 5.32 (s, 4H, ^2J(Pt–CH=) = 45.7 Hz), 2.41–2.25 (m, 8H), 1.09 (s, 12H).

The alkylchloro complexes [(COD)PtRCl] for comparison to the products from photolysis reactions in CD_2Cl_2 have been generated following the method by Clark and Manzer for [(COD)PtMeCl] [1].

4.3. Theoretical calculations

Ground state electronic structure calculations on complexes [(COD)Pt(R)$_2$] have been done on the base of DFT methods using the ADF1999 [36,37] and GAUSSIAN 98 [38] program packages. The lowest excited states of the closed shell complexes were calculated by the time-dependent DFT (TD DFT) method (both ADF and G98 programs).

Within the ADF program, Slater type orbital (STO) basis sets of triple-ζ quality with polarization functions were employed. The inner shells were represented by frozen core approximation (1s for C, and 1s–4d for Pt were kept frozen). The following density functionals were used within ADF: the local density approximation (LDA) with VWN parametrization of electron gas data or the functional including Becke's gradient correction [39] to the local exchange expression in conjunction with Perdew's gradient correction [40] to the LDA expression (ADF/BP). The scalar relativistic zero order regular approximation (ZORA) was used within this study.

Within GAUSSIAN 98, Dunning's polarized valence double-ζ basis sets [41] were used for C and H atoms and the quasirelativistic effective core pseudopotentials and corresponding optimized set of basis functions [42] for Pt. Hybrid Becke's three parameter functional with Lee, Yang and Parr correlation functional (B3LYP) [43] was used in GAUSSIAN 98 calculations (G98/B3LYP). The calculations on [(COD)Pt(Ph)$_2$] were performed in C_2 constrained symmetry. C_{2v} constrained symmetry was utilized within other [(COD)Pt(R)$_2$] systems, with the z axis coincident with C_2 symmetry axis and the central atoms of the R substituents in the yz plane. All results discussed correspond to optimized geometries.

Acknowledgements

This work was carried out within the scope of the COST D14 action. A.K. would like to thank Professor D.J. Stufkens (University of Amsterdam) for the opportunity to do research in his group, for fruitful discussions and financial support. Professor W. Kaim is also acknowledged for financial support as well as Johnson Matthey PLC ('JM') for a loan of K_2PtCl_4. S.Z. thanks also for the financial support from the Ministry of Education of the Czech Republic (OC.D14.20).

References

[1] H.C. Clark, L.E. Manzer, J. Organomet. Chem. 59 (1973) 411.
[2] C.R. Kistner, J.H. Hutchinson, J.R. Doyle, J.C. Storlie, Inorg. Chem. 2 (1963) 1255.
[3] M.W. Holtcamp, J.A. Labinger, J.E. Bercaw, Inorg. Chim. Acta 265 (1997) 117.
[4] Z. Dawoodi, C. Eaborn, A. Pidcock, J. Organomet. Chem. 170 (1979) 95.
[5] N. Chaudhury, R.J. Puddephatt, J. Organomet. Chem. 84 (1975) 105.
[6] G.K. Anderson, H.C. Clark, J.A. Davies, Inorg. Chem. 20 (1981) 1636.
[7] B.C. Ankianiec, G.B. Young, Polyhedron 8 (1989) 57.
[8] K.A. Fallis, G.K. Anderson, N.P. Rath, Organometallics 12 (1993) 2435.
[9] M. Bochmann, G. Wilkinson, G.B. Young, J. Chem. Soc. Dalton Trans. (1980) 1879.
[10] T.R. Lee, G.M. Whitesides, J. Am. Chem. Soc. 113 (1991) 2576.
[11] R. Kumar, S. Roy, M. Rashidi, R.J. Puddephatt, Polyhedron 8 (1989) 551.
[12] H. Kunkely, A. Vogler, J. Organomet. Chem. 553 (1998) 517.
[13] D.-S. Yang, G.M. Bancroft, L. Dignard-Bailey, R.J. Puddephatt, J.S. Tse, Inorg. Chem. 29 (1990) 2487.
[14] D.-S. Yang, G.M. Bancroft, R.J. Puddephatt, J.S. Tse, Inorg. Chem. 29 (1990) 2496.
[15] D.-S. Yang, G.M. Bancroft, R.J. Puddephatt, K.H. Tan, J.N. Cutler, J.D. Bozek, Inorg. Chem. 29 (1990) 4956.
[16] A.C. Balazs, K.H. Johnson, G.M. Whitesides, Inorg. Chem. 21 (1982) 2162.
[17] J. Müller, P. Göser, Angew. Chem. Int. Ed. Engl. 8 (1967) 380.
[18] T.M. Miller, G.M. Whitesides, J. Am. Chem. Soc. 110 (1988) 3164.
[19] P. Foley, R. DiCosimo, G.M. Whitesides, J. Am. Chem. Soc. 102 (1980) 6713.
[20] M. Hackett, G.M. Whitesides, J. Am. Chem. Soc. 110 (1988) 1449.
[21] D.C. Griffiths, G.B. Young, Organometallics 8 (1989) 875.
[22] B. Wozniak, J.D. Ruddick, G. Wilkinson, J. Chem. Soc. A (1971) 3116.
[23] R. Wyrwa, W. Poppitz, H. Görls, Z. Allg. Anorg. Chem. 623 (1997) 649.
[24] E. Costa, P.G. Pringle, M. Ravetz, Inorg. Synth. 31 (1997) 284.
[25] L.R. Falvello, S. Fernandez, J. Fornies, E. Lalinde, F. Martinez, M.T. Moreno, Organometallics 16 (1997) 1326.
[26] R.J. Cross, M.F. Davidson, J. Chem. Soc. Dalton Trans. (1986) 1987.
[27] C. Eaborn, K.J. Odell, A. Pidcock, J. Chem. Soc. Dalton Trans. (1978) 357.
[28] A. Klein, K.-W. Klinkhammer, T. Scheiring, J. Organomet. Chem. 592 (1999) 128.
[29] G.B. Deacon, E.A. Hilderbrand, E.R.T. Tiekink, Z. Kristallogr. 205 (1993) 340.
[30] H. Palkovits, U. Ziegler, G. Schmidtberg, H.-A. Brune, J. Organomet. Chem. 338 (1988) 119.
[31] H.-A. Brune, R. Hohenadel, G. Schmidtberg, U. Ziegler, J. Organomet. Chem. 402 (1991) 179.
[32] R. Klotzbücher, H.-A. Brune, J. Organomet. Chem. 299 (1986) 399.
[33] P.S. Braterman, R.J. Cross, G.B. Young, J. Chem. Soc. Dalton Trans. (1977) 1892.
[34] H.-A. Brune, U. Mayr, G. Schmidtberg, Z. Naturforsch. 41b (1986) 1281.
[35] P.S. Braterman, Top. Curr. Chem. 92 (1980) 149.
[36] C. Fonseca Guerra, J.G. Snijders, G. te Velde, E.J. Baerends, Theor. Chim. Acta 99 (1998) 391.
[37] E.J. Baerends, A. Bérces, C. Bo, P.M. Boerrigter, L.Cavallo, L. Deng, R.M. Dickson, D.E. Ellis, L. Fan, T.H. Fischer, C. Fonseca Guerra, S.J.A. Van Gisbergen, J.A. Groeneveld, O.V. Gritsenko, F.E. Harris, P. van den Hoek, H. Jacobsen, G. van Kessel, F. Kootstra, E. van Lenthe, V.P. Osinga, P.H.T. Philipsen, D. Post, C.C. Pye, W. Ravenek, P. Ros, P.R.T. Schipper, G. Schreckenbach, J.G. Snijders, M. Sola, D. Swerhone, G. te Velde, P. Vernooijs, L. Versluis, V. Visser, E. van Wezenbeek, G. Wiesenekker, S.K. Wolff, T.K. Woo, T. Ziegler, ADF 1999.01, Amsterdam, 1999.
[38] M.J. Frisch, G.W. Trucks, H.B. Schlegel, G.E. Scuseria, M.A. Robb, J.R. Cheeseman, V.G. Zakrzewski, Jr., J.A. Montgomery, R.E. Stratmann, J.C. Burant, S. Dapprich, J.M. Millam, A.D. Daniels, K.N. Kudin, M.C. Strain, O. Farkas, J. Tomasi, V. Barone, M. Cossi, R. Cammi, B. Mennucci, C. Pomelli, C. Adamo, S. Clifford, J. Ochterski, G.A. Petersson, P.Y. Ayala, Q. Cui, K. Morokuma, D.K. Malick, A.D. Rabuck, K. Raghavachari, J.B. Foresman, J. Cioslowski, J.V. Ortiz, A.G. Baboul, B.B. Stefanov, G. Liu, A. Liashenko, P. Piskorz, I. Komaromi, R. Gomperts, R.L. Martin, D.J. Fox, T. Keith, M.A. Al-Laham, C.Y. Peng, A. Nanayakkara, C. Gonzalez, M. Challacombe, P.M.W. Gill, B. Johnson, W. Chen, M.W. Wong, J.L. Andres, C. Gonzalez, M. Head-Gordon, E.S. Replogle, J.A. Pople, GAUSSIAN 98, Revision A.7; Gaussian Inc., Pittsburgh PA, 1998.
[39] A.D. Becke, Phys. Rev. A 38 (1988) 3098.
[40] J.P. Perdew, Phys. Rev. A 33 (1986) 8822.
[41] P.J. Stephens, F.J. Devlin, C.F. Cabalowski, M.J. Frisch, J. Phys. Chem. 98 (1994) 11623.
[42] D.E. Woon, T.H.J. Dunning, J. Chem. Phys. 98 (1993) 1358.
[43] D. Andrae, U. Häussermann, M. Dolg, H. Stoll, H. Preuss, Theor. Chim. Acta 77 (1990) 123.